

H/C elemental ratio of the refractory organic matter in cometary particles of 67P/Churyumov-Gerasimenko

R. Isnard^{1,2}, A. Bardyn³, N. Fray¹, C. Briois², H. Cottin¹, J. Paquette⁴, O. Stenzel⁴, C. Alexander³, D. Baklouti⁵, C. Engrand⁶, F.-R. Orthous-Daunay⁷, S. Siljeström⁸, K. Varmuza⁹, and M. Hilchenbach⁴

¹ Laboratoire Interuniversitaire des Systèmes Atmosphériques, UMR CNRS 7583, Université Paris Est Créteil (UPEC) et Université Paris Diderot (UPD), Créteil, France
e-mail: robin.isnard@lisa.u-pec.fr

² Laboratoire de Physique et Chimie de l'Environnement et de l'Espace, UMR CNRS 7328, Université d'Orléans et du CNES, Orléans, France

³ DTM, Carnegie Institution of Washington, Washington, DC, USA

⁴ MPS, Justus-von-Liebig-Weg 3, 37077 Göttingen, Germany

⁵ Institut d'Astrophysique Spatiale, CNRS/Université Paris-Sud, Université Paris-Saclay, bâtiment 121, Université Paris-Sud, 91405 Orsay Cedex, France

⁶ CSNSM, CNRS-IN2P3, Université Paris-Sud, Université Paris-Saclay, Bâtiment 104, 91405 Orsay Campus, France

⁷ Univ. Grenoble Alpes, CNRS, CNES, IPAG, 38000 Grenoble, France

⁸ Bioscience and Materials / Chemistry and Materials, RISE Research Institutes of Sweden, Stockholm, Sweden

⁹ Institute of Statistics and Mathematical Methods in Economics, Vienna University of Technology, Wiedner Hauptstrasse 7/105-6, 1040 Vienna, Austria

Received 7 December 2018 / Accepted 5 March 2019

ABSTRACT

Context. Because comets are part of the most primitive bodies of our solar system, establishing their chemical composition and comparing them to other astrophysical bodies gives new constraints on the formation and evolution of organic matter throughout the solar system. For two years, the time-of-flight secondary ion mass spectrometer COmetary Secondary Ion Mass Analyzer (COSIMA) on board the Rosetta orbiter performed in situ analyses of the dust particles ejected from comet 67P/Churyumov-Gerasimenko (67P).

Aims. The aim is to determine the H/C elemental ratio of the refractory organic component contained in cometary particles of 67P.

Methods. We analyzed terrestrial and extraterrestrial calibration samples using the COSIMA ground-reference model. Exploiting these calibration samples, we provide calibration lines in both positive and negative ion registration modes. Thus, we are now able to measure the cometary H/C elemental ratio.

Results. The mean H/C value is 1.04 ± 0.16 based on 33 different cometary particles. Consequently, the H/C atomic ratio is on average higher in cometary particles of 67P than in even the most primitive insoluble organic matter extracted from meteorites.

Conclusions. These results imply that the refractory organic matter detected in dust particles of 67P is less unsaturated than the material in meteorites.

Key words. comets: individual: 67P/Churyumov-Gerasimenko – astrochemistry

1. Introduction

Comets are small bodies that are thought to have formed in the early protoplanetary disk. They are believed to contain unmodified materials since their formation (Willacy et al. 2015). For this reason, studying them helps to decipher the physical and chemical conditions that prevailed during planetesimal formation at about 4.6 billion years ago. In particular, investigating cometary dust composition provides new constraints on the history of comets and the formation of the solar system.

In 1986, PIA, PUMA-1, and PUMA-2 were the first mass spectrometers to perform in situ analyses of cometary particles during the flyby of comet 1P/Halley by the *Giotto*, Vega-1, and Vega-2 spacecrafts (Kissel et al. 1986a,b). The mass spectra revealed that cometary matter is composed of minerals and organics, the latter being mainly made of C, H, O, and N atoms (Kissel et al. 1986a,b; Clark et al. 1987; Jessberger et al. 1988; Lawler & Brownlee 1992). The cometary organic

matter was particularly difficult to characterize because of the high-velocity impacts (about 70 km s^{-1}) of the particles, releasing mostly mono-atomic ions rather than polyatomic ions (Kissel & Krueger 1987). However, possible molecular identifications have been proposed (Kissel & Krueger 1987; Fomenkova et al. 1994; Fomenkova 1999). The average elemental composition for the dust determined by Jessberger et al. (1988) shows that the carbon-to-magnesium ratio was about ten times higher in the particles of 1P/Halley than in CI carbonaceous chondrites, demonstrating that comets are among the most carbon-rich bodies of the solar system.

In 2006, the Stardust mission for the first time brought cometary samples back to Earth that were collected in the coma of comet 81P/Wild 2 (Brownlee et al. 2006). Laboratory analyses of these cometary particles detected rather faint organic signatures (Cody et al. 2008; Elsila et al. 2009; Bajt et al. 2009), but an accurate characterization remained challenging because of the high-impact speed (about 6 km s^{-1}) of the particles that were

collected in the aerogel and organic-rich content of the aerogel itself (Sandford et al. 2010; Brownlee 2014). However, De Gregorio et al. (2011) suggested that one unaltered collected particle may contain a highly aromatic material and a refractory organic component resembling the insoluble organic matter (IOM) extracted from meteorites.

Cometary organic matter can also be characterized by studying extraterrestrial samples such as cosmic dust particles collected in the Earth's stratosphere and in Antarctic snow (Brownlee 2016; Flynn et al. 2016; Sandford et al. 2016; Duprat et al. 2010, and references therein). More specifically, chondritic porous anhydrous interplanetary dust particles (CP-IDPs) and ultracarbonaceous Antarctic micrometeorites (UCAMMs) are believed to originate from comets. Their carbon contents are higher than those of carbonaceous chondrites (Thomas et al. 1993; Dartois et al. 2018). Analyses have shown that the organic matter of IDPs contains unsaturated material characterized by C=C functions and CH aliphatic signatures (Flynn et al. 2003). In UCAMMs, the organic matter is dominated by polyaromatic matter, with a low O content and variable aliphatic CH signatures. Aromatic CH is also sometimes detected in UCAMMs (Dartois et al. 2018).

Between August 2014 and September 2016, the ESA Rosetta space mission has investigated comet 67P/Churyumov-Gerasimenko (hereafter 67P) through in situ measurements, providing new constraints on the origin and evolution of comets. Located on board the Rosetta orbiter, the COMetary Secondary Ion Mass Analyzer (COSIMA) instrument was a time-of-flight secondary ion mass spectrometer (TOF-SIMS) designed to analyze the chemical composition of the cometary dust ejected from the nucleus of 67P (Hilchenbach et al. 2016; Kissel et al. 2007). It has been shown based on the mass spectra measured by COSIMA that the cometary particles contain organic matter that is different from all the well-characterized organic compounds analyzed during the calibration phase on ground (such as carboxylic acids, amino acid, nucleobases, hydrocarbons, and polycyclic aromatic hydrocarbons, PAHs; Le Roy et al. 2015a; Fray et al. 2016). A pronounced spectral feature of the cometary organic component is that the most abundant organic fragments are at low masses: C⁺, CH⁺, CH₂⁺, CH₃⁺, and C₂H₃⁺ (Fray et al. 2016). These first results also demonstrated that the spectra of the cometary particles resemble the spectral signature of the IOM extracted from carbonaceous chondrites. Thus, cometary particles of 67P contain organic matter with high molecular weight. Additionally, the N/C atomic ratio of the refractory organic matter was recently determined by Fray et al. (2017) and confirmed the chemical similarities with chondritic IOM. Moreover, Bardyn et al. (2017) showed that the cometary particles are among the most carbon-rich objects in the solar system, containing about 50% by mass of organic matter. At the time, the elemental H/C ratio of the refractory organic matter was not known, and a ratio of 1 was assumed in order to determine the elemental composition of the cometary particles of 67P (Bardyn et al. 2017). In this paper, the H/C ratio is determined and the implications are discussed.

The H/C atomic ratio in extraterrestrial samples, such as chondrites, micrometeorites, and IDPs, are available in the literature. H/C values measured on bulk meteorites do not only represent the organic fraction of the material, but may also include the contribution of hydrated minerals and carbonates (Alexander et al. 2012). IOM, extracted from meteorites by demineralization with HF or CsF, is a highly cross-linked macromolecular material (Cody et al. 2002; Derenne & Robert 2010; Quirico et al. 2014) and is free of water and carbonates. Because

the COSIMA mass spectra of the 67P cometary particles do not show signatures from hydrated minerals (Bardyn et al. 2017) and carbonates, the H/C atomic ratio of the particles must be related to the organic material, which is thought to be refractory and comparable to the IOMs extracted from meteorites (Fray et al. 2016). Alexander et al. (2007, 2010, 2014) reported a wide range of H/C values from around 0.1 up to almost 1 for IOMs extracted from various types of chondrites. Much of this variation is due to modification in the chondrite parent bodies during aqueous alteration and thermal metamorphism. The H/C atomic ratio in the particles of 81P/Wild2 brought back to Earth by the Stardust mission could not be quantified because of the interference of organic compounds in the aerogel that collected the particles (Sandford et al. 2010). A cometary value of H/C = 2.49 ± 0.98 was obtained by Jessberger et al. (1988), who measured the average atomic abundances of elements in Halley's dust. For the organic component of cometary particles of comet Halley, Kissel & Krueger (1987) have estimated a H/C elemental ratio of 0.8. However, the hydrogen quantification from the PUMA-1 mass spectrometer is highly uncertain (see discussion in Kissel & Krueger 1987).

Here we report for the first time the H/C atomic ratio of 33 cometary particles collected in the coma of 67P. These values are compared with those measured in comets and other extraterrestrial bodies, highlighting the similarities and the differences.

2. Methods

2.1. COSIMA instrument

For two years, the time-of-flight secondary ion mass spectrometer COSIMA on board the Rosetta orbiter collected, imaged, and analyzed in situ the composition of cometary particles of 67P. Details regarding the technical features of this instrument are available in Kissel et al. (2007). The cometary particles studied here were collected on target plates of 10 × 10 mm² that were covered by a fluffy gold layer (Hornung et al. 2014). The targets were exposed on movable target holders that could be placed in front of a funnel in such a way that the cometary dust that entered the instrument was focused onto the collection target. The impact velocity of the particles was not higher than 10 m s⁻¹ (Rotundi et al. 2015), which is much lower than the collection velocity of 6 km s⁻¹ during the Stardust mission (Brownlee et al. 2006) and the encounter speeds of about 78 and 68 km s⁻¹ estimated for the Vega (Sagdeev et al. 1986) and Giotto (Reinhard 1986) spacecrafts, respectively. Considering this low capture velocity, the chemical composition of particles of 67P is very probably not altered by the capture process.

After they were collected, the particles were first imaged by an internal optical microscope called COSISCOPE, whose spatial resolution is 14 μm (Hornung et al. 2016; Langevin et al. 2016). Then, some particles were analyzed by TOF-SIMS with a beam of ¹¹⁵In⁺. This primary ion beam was generated by a liquid indium ion source with an energy of 8 keV and was pulsed (around 1000 ions per pulse within 3 ns with a 1.5 kHz repetition rate) and focused to give a footprint of 35 × 50 μm² (full width at half-maximum) on the target (Hilchenbach et al. 2016; Kissel et al. 2007). The primary ¹¹⁵In⁺ ions eject neutrals and secondary ions from the surface of the sample. The latter were collected and accelerated into a reflectron TOF system. The collected secondary ions are either positive or negative, depending on the acceleration voltage. The times-of-flight of the secondary ions were measured and then converted into mass over charge (*m/z*) ratios, generating a mass spectrum with a mass

Table 1. Characteristics of the calibration samples analyzed with the COSIMA RM.

#	Name	Target	Classification	H/C (at.)	Reference	H ⁺ /C ⁺	H ⁻ /C ₂ ⁻	Analysis date (+)	Analysis date (-)
1	Kerogen	556	type III	0.75 ± 0.03	Piani (2012)	4.98 ± 0.02	52.0 ± 0.1	2017-06-14	2017-06-11
2	IOM Orgueil	556	CII	0.673 ± 0.014	Alexander et al. (2007)	4.89 ± 0.07	42.2 ± 9.9	2017-06-13	2017-06-10
3	IOM EET 92042	574	CR2	0.757 ± 0.02	Alexander et al. (2007)	5.49 ± 0.04	23.4 ± 0.5	2018-02-12	2017-11-09
4	IOM GRO 95566	574	CM2	0.665 ± 0.005	Alexander et al. (2010)	5.05 ± 0.09	23.6 ± 1.0	2018-02-12	2017-11-09
5	IOM GRO 95577	574	CR1	0.786 ± 0.031	Alexander et al. (2007)	4.40 ± 0.07	18.5 ± 2.4	2018-02-12	2018-02-13
6	IOM PCA 91008	574	CM _{heated}	0.242	Alexander et al. (2010)	2.84 ± 0.09	15.4 ± 2.4	2018-02-12	2017-11-09
7	IOM Tagish Lake 1	575	C2, ungrouped	0.337 ± 0.01	Alexander et al. (2007)	3.10 ± 0.07	15.6 ± 1.1	2018-02-11	2018-02-11
8	IOM Tagish Lake 3	575	C2, ungrouped	0.509 ± 0.025	Alexander et al. (2014)	4.07 ± 0.08	21.8 ± 1.2	2018-02-11	2018-02-12
9	IOM Tagish Lake 4	575	C2, ungrouped	0.594	Alexander et al. (2014)	4.14 ± 0.09	36.0 ± 5.7	2018-02-11	2018-02-12
10	IOM Tagish Lake 5	575	C2, ungrouped	0.722 ± 0.063	Alexander et al. (2014)	5.00 ± 0.09	30.6 ± 2.9	2018-02-11	2018-02-12
11	Coronene	56E	PAH (C ₂₄ H ₁₂)	0.5	–	4.28 ± 0.01	39.2 ± 7.8	2018-03-09	2018-03-09
12	Diamond	56E	–	0	–	2.37 ± 0.02	16.8 ± 4.0	2018-03-09	2018-03-09
13	Graphite	56E	–	0	–	2.77 ± 0.02	12.1 ± 0.3	2018-03-09	2018-03-09
14	Hexatriacontane	56E	alkane (C ₃₆ H ₇₄)	2.055	–	11.78 ± 0.06	181 ± 17	2018-03-09	2018-03-09

Notes. Columns are: target numbers, the H/C atomic ratio from the literature, the measured H⁺/C⁺ and H⁻/C₂⁻ ion ratios and the analysis dates for both secondary ion registration modes.

resolution $m/\Delta m$ of about 1400 (full width at half-maximum) at $m/z = 100$ (Hilchenbach et al. 2016). At a given integer mass for $m/z < 100$, this resolution is enough to separate elemental ions from hydrogen-containing organic ions. All the mass spectra presented here have been measured with an acquisition time of 2.5 min, corresponding to 225 000 individual primary ion beam shots. Presputtering, which is a common preparation procedure on samples analyzed in the laboratory by TOF-SIMS, was not performed on any of the particles studied in this paper in order to save the primary indium source during the two-year Rosetta mission. Since the COSIMA instrument did not have an electron flood gun, the charging of the cometary particles through implantation of primary ¹¹⁵In⁺ ions could not be compensated for. More than 35 000 cometary particles and particle fragments were collected and imaged by COSIMA (Merouane et al. 2017), but because the amount of indium available for the whole mission was limited, only about 250 were analyzed by TOF-SIMS in both positive and negative secondary ion registration modes. Their individual size varies from 14 to 800 μm (Langevin et al. 2016). The Micro-Imaging Dust Analysis System (MIDAS) instrument observed subunits smaller than 2.5 μm , which is similar to those found in IDPs and micrometeorites (Bentley et al. 2016). Given the size of the primary ion beam of COSIMA (about $35 \times 50 \mu\text{m}^2$), the analyses are always mixtures of minerals and organics (Bardyn et al. 2017).

2.2. Calibration samples

The H/C ratio can be estimated by SIMS and NanoSIMS techniques through the intensity measurements of H⁺ and C⁺ (Le Guillou et al. 2013) or H⁻ and C⁻ (Carrasco et al. 2016; Aléon et al. 2001), which yield the H⁺/C⁺ and H⁻/C⁻ ion ratios, respectively. These ionic ratios are considered to be directly proportional to the elemental H/C ratio. Therefore, here we search for relationships between the H/C elemental ratio and any relevant ionic ratios.

To determine the H/C atomic ratio of the cometary particles, we have analyzed calibration samples with known H/C ratios using a ground-based reference model (RM) that was identical to the flight model (XM) of COSIMA. In our case, we chose samples of IOM extracted from carbonaceous chondrites

by a CsF-HF demineralization technique (Alexander et al. 2007; Cody et al. 2002), one kerogen (type III) extracted from a sedimentary rock, and other carbonaceous compounds such as graphite (Aldrich), diamond (Aldrich), hexatriacontane (Aldrich, 98% purity), and coronene (Fluka, 98% purity; see Table 1). As the carbonaceous component of the cometary particles of 67P is dominated by organic matter with a high molecular weight that resembles the IOMs extracted from chondrites (Fray et al. 2016), we considered several samples of chondritic IOMs (see Table 1). Kerogens are organic materials extracted from terrestrial rocks. Like IOMs, they are composed of a complex mixture of insoluble macromolecules containing aromatic and aliphatic moieties. We then also studied a sample of type III kerogen. Whereas pure samples of hexatriacontane, coronene, graphite, and diamond cannot be considered good analogs of the cometary organic matter, they were selected to study the spectral signatures of their respective chemical family (alkanes, PAHs, and pure carbon samples). These four samples are mainly assumed to represent the end members of the calibration curves and are thought to be useful to search for a potential relationship between some ionic ratios and the chemical structure. All samples were pressed using a sapphire window into blank gold targets that were previously cleaned with at least 98% purity solvents (acetone and hexane) and either preheated at 900°C for 10 min (targets 556 and 56E, see Table 1) or stored in a vacuum chamber for two days (targets 574 and 575, see Table 1) in order to remove the most volatile organic contaminants. Table 1 summarizes the H/C atomic ratios (ranging from 0 to 2.055) of the 14 samples.

Because TOF-SIMS is a surface-sensitive technique, the possibility of surface contamination must always be borne in mind. For each calibration sample that was analyzed with the RM, we therefore only kept the spectra that showed the lowest intensities of gold, polydimethylsiloxane (PDMS), and fluorinated fragments in both positive and negative ion registration modes. PDMS is a contaminant that is often observed in TOF-SIMS analyses (Vickerman & Briggs 2013; Henkel & Gilmour 2014). However, fluorine contamination was also observed in some IOM samples. In these samples, we generally observe both a spatially homogeneous source of fluorine and highly localized sources (see Fig. A.1). The C⁺ signal is strongly enhanced in

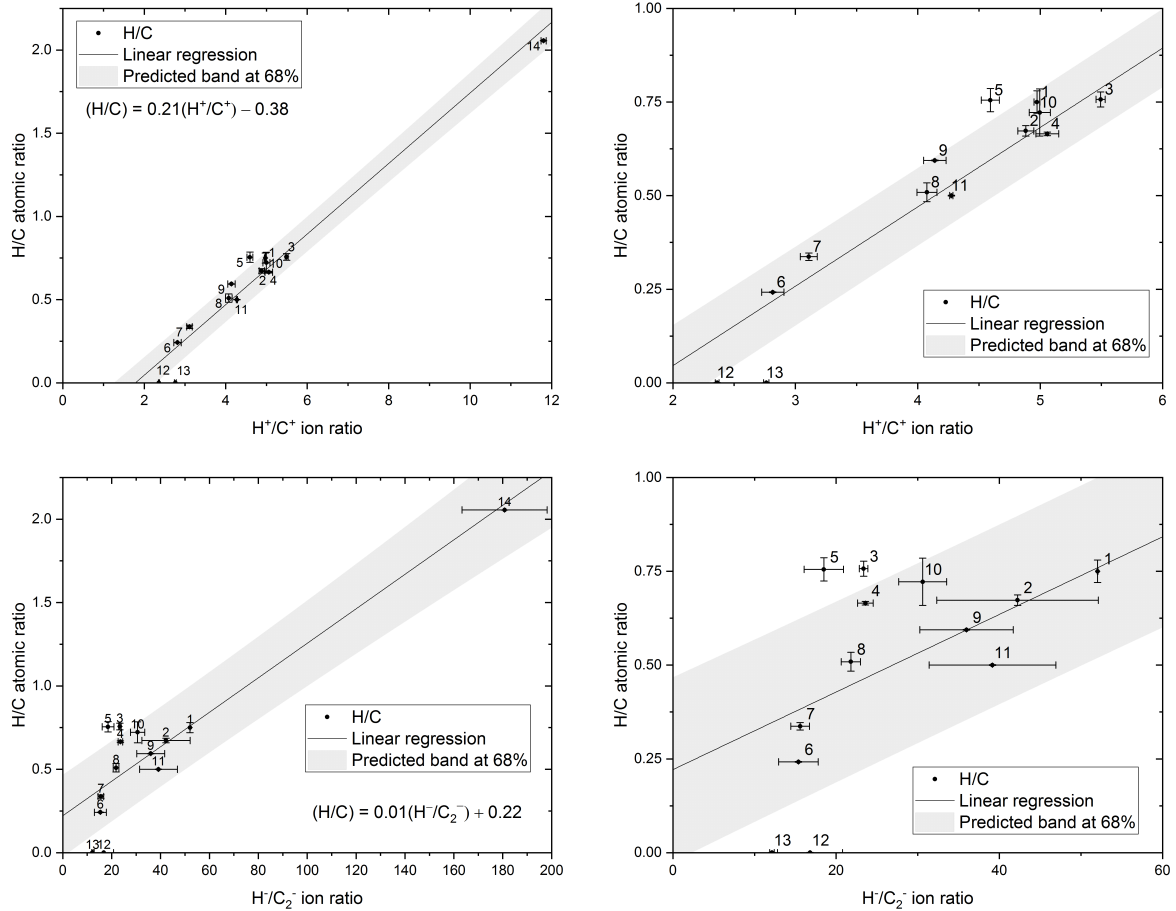


Fig. 1. Calibration curves of the H/C atomic ratio as a function of the H^+/C^+ (top left panel) and H^-/C_2^- (bottom left panel) ion ratios. The black dots refer to the 14 calibration samples with their corresponding number (see Table 1). Right panels: enlargements of their respective left panel. The black line is the linear regression and the grey zone represents the predicted confidence band at 68%.

highly contaminated regions of the sample, suggesting that it is organofluorine (Fig. A.1). For this reason, we only considered the analysis performed on the noncontaminated areas of the IOM samples in order to obtain representative mass spectra. Even by doing so, fragment ions of PDMS (mainly $Si(CH_3)_3^+$ and $Si_2O(CH_3)_5^+$ in positive mode and CH_3SiO^- and $CH_3SiO_2^-$ in negative mode) are still observed in the final selection, although their intensities are much lower (at least by a factor of 5) than the values in the spectra acquired on the gold target. Therefore the intensity of each individual ion fragment of interest must be corrected by removing the contribution of PDMS using the Eq. (1):

$$X = X_{\text{sample}} - (X_{\text{target}} \times f). \quad (1)$$

In Eq. (1), X_{sample} (or X_{target}) represents the number of counts of a specific ion that is ejected from the sample (or from the target). The normalization factor f corresponds to the mean ratio between the ratios of intensities of the PDMS fragments coming from the sample and the target. Mathematically speaking, f is calculated with Eq. (2) (or Eq. (3)) for positive (or negative) ions:

$$f = \left(\frac{[Si(CH_3)_3^+]_{\text{sample}}}{[Si(CH_3)_3^+]_{\text{target}}} + \frac{[Si_2O(CH_3)_5^+]_{\text{sample}}}{[Si_2O(CH_3)_5^+]_{\text{target}}} \right) / 2, \quad (2)$$

$$f = \left(\frac{[CH_3SiO^-]_{\text{sample}}}{[CH_3SiO^-]_{\text{target}}} + \frac{[CH_3SiO_2^-]_{\text{sample}}}{[CH_3SiO_2^-]_{\text{target}}} \right) / 2. \quad (3)$$

The same type of correction has previously been used to handle the COSIMA positive (Bardyn et al. 2017) and negative

(Fray et al. 2017) spectra. For each X value, we assigned an error bar that took the error in the normalization factor f into account. This error bar is not related to the counting statistics. Then, considering another Y ion count, the uncertainty on a X/Y ion ratio was estimated from the individual errors of X and Y ions.

To deduce the H/C atomic ratio of the cometary particles, we have to find correlations between the known H/C elemental ratio of standards and some defined ionic ratios measured on the standards (see Table 1). Numerous ion ratios have been tested in both ionization registration modes, including H^+/C^+ , CH^+/C^+ , CH_3^+/C^+ and H^-/C^- , H^-/C_2^- , C_2H^-/C_2^- and many others involving low-mass ($m/z < 26$) hydrocarbon ions. For each ionization mode, we only used the ion ratio that produced the highest correlation coefficient (i.e., R^2) with the known H/C elemental ratios. We found that the H^+/C^+ and H^-/C_2^- ratios produced the best linear fits with an R^2 equal to 0.96 and 0.79, respectively. Figure 1 shows the two selected calibration lines with their respective equations. From the values of R^2 and the apparent widths of the predicted band at 68% (1σ standard deviation), it is clear that the dispersion within the H^-/C_2^- calibration is higher than that within the H^+/C^+ calibration. Nevertheless, both calibration curves were used to measure the H/C atomic ratio of the cometary organic matter. All other things being equal, the two lines are expected to give similar values for the H/C.

As shown in Bardyn et al. (2017), the cometary particles are extremely rich in organic matter. On average, the latter represents almost 50% of the particles masses, meaning that about 70% of the particle volume is composed of organic material. An ideal

analog of the cometary particles should contain the same large amount of carbonaceous IOM-like material mixed, at the micron scale, to silicates and other minerals. It is not trivial to prepare and obtain such a representative analog. However, a pure IOM extracted from a carbonaceous chondrite is clearly a more suitable cometary analog than the carbonaceous chondrite itself. The organic content of a carbonaceous chondrite represents less than 10% of its mass, and its hydrogen comes mainly from phyllosilicates. In addition, carbon being a minor element in carbonaceous chondrites, the organic matter is a smaller component trapped in a mineral matrix. In this case, TOF-SIMS yields for H and C could probably be noticeably affected by the surrounding matrix and thus different from the yields measured on the cometary particles. The H/C calibration lines of this paper were obtained from almost pure carbonaceous samples, implying that any possible effect of the minerals on the SIMS yields of C^+ , H^+ , C_2^- and H^- should be limited in the cometary particles and within the error bars of the curves obtained.

2.3. COSIMA mass spectra of the cometary particles

Throughout the Rosetta mission, cometary particles have been analyzed, some even several times. To investigate the H/C of a individual cometary particle in both ion registration modes, we need to select analyses that have been performed within the same period of time in both modes. By doing so, the studied measurements are less affected by potential bias that is due to instrumental instability over time. However, the exact same spatial location for both modes cannot be guaranteed because the precise position of the ion beam may vary by up to $30\ \mu\text{m}$ from one mode to the other. Moreover, the ion beam is large enough ($35 \times 50\ \mu\text{m}^2$ at FWHM) for all the acquired mass spectra of cometary particles to always contain a contribution of the PDMS coming from the gold target. Additionally, the PDMS contamination level is higher in the spectra performed on target than on particles. Thus, our spatial selection is mainly based on the less strongly PDMS-contaminated analyses, in the same way as we selected spectra from the calibration samples.

Using this method, we obtained 35 different analyses (see Table B.1) with similar the acquisition dates for the positive and negative ionization modes. These 35 analyses correspond to 33 different particles because two of them (Bonin and Umeka) were analyzed twice to test the reproducibility of the measurements. In positive and in negative modes, background spectra were obtained from the gold target adjacent to the particles and on the same date. The PDMS ions counts in these background spectra are higher than in the spectra of cometary particles. Figure 2 displays the usual cometary (without correction) and background signatures in positive and negative registration modes, here shown for particle Fred. For the negative-mass spectra obtained on cometary particles, we observe for some peaks a long shoulder toward the left-hand side of the main peak. Some examples are shown in Fig. 2 of Fray et al. (2017). This feature is explained by the fact that the surface of the cometary particles is positively charged as a result of the implantation of In^+ primary ions (Hilchenbach et al. 2017, Hornung et al. in prep.). This effect is not expected to affect the H^-/C_2^- ionic ratio. Moreover, it is only observed in the spectra acquired on the cometary particles and not in the spectra performed on the conductive gold target, so that it can be used as an indication of whether a given ion originated from the particle or the target. For all the cometary spectra, H^- , C_2^- , $\text{CH}_3\text{SiO}_2^-$, and $\text{CH}_3\text{SiO}_2^-$ peaks were integrated over their whole width, including the left-hand shoulder if present.

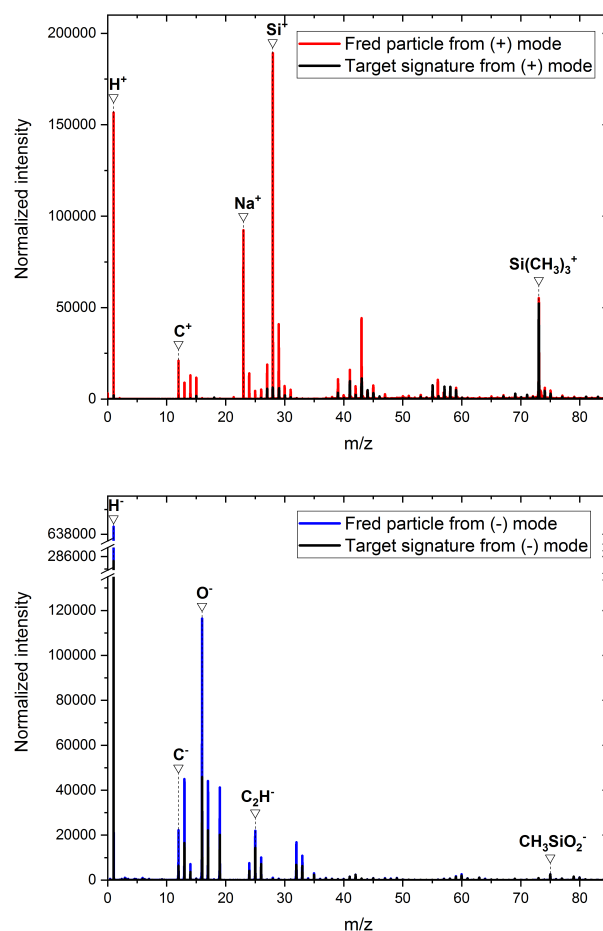


Fig. 2. Mass spectra of the cometary particle Fred and the related target in both positive (*top panel*) and negative (*bottom panel*) ionization registration modes. The intensity is normalized to the $\text{Si}(\text{CH}_3)_3^+$ and $\text{CH}_3\text{SiO}_2^-$ fragments in each panel.

As for calibration samples, we chose to correct the number of counts of a specific ion using Eq. (1). The resulting values of the H^+/C^+ and H^-/C_2^- ratios for the cometary particles are listed in Table B.1.

3. Results and discussion

3.1. H/C atomic ratios of the cometary particles

From the calibrations and measurements of H^+/C^+ and H^-/C_2^- ratios, we calculated two values of the elemental H/C ratio for each analysis, corresponding to the two ionization registration modes (see Table B.1 and Fig. 3). The mean values are 0.97 ± 0.15 and 1.12 ± 0.14 for the positive and negative ion modes (the error bars represent the 1σ standard deviation), respectively. Considering the 70 different individual elemental H/C ratios in the two ion registration modes, we can estimate an average cometary H/C atomic ratio of 1.04 ± 0.16 , the error bar being the 1σ standard deviation.

The particles Bonin and Umeka were analyzed at two different periods, producing a total of four measurements for each particle. While the Bonin H/C measurements are consistent within and between the two ionization registration modes, the H/C values of Umeka differs from one mode to the other. One explanation could be that we did not probe exactly the same part of the cometary particle when we analyzed it with the two modes.

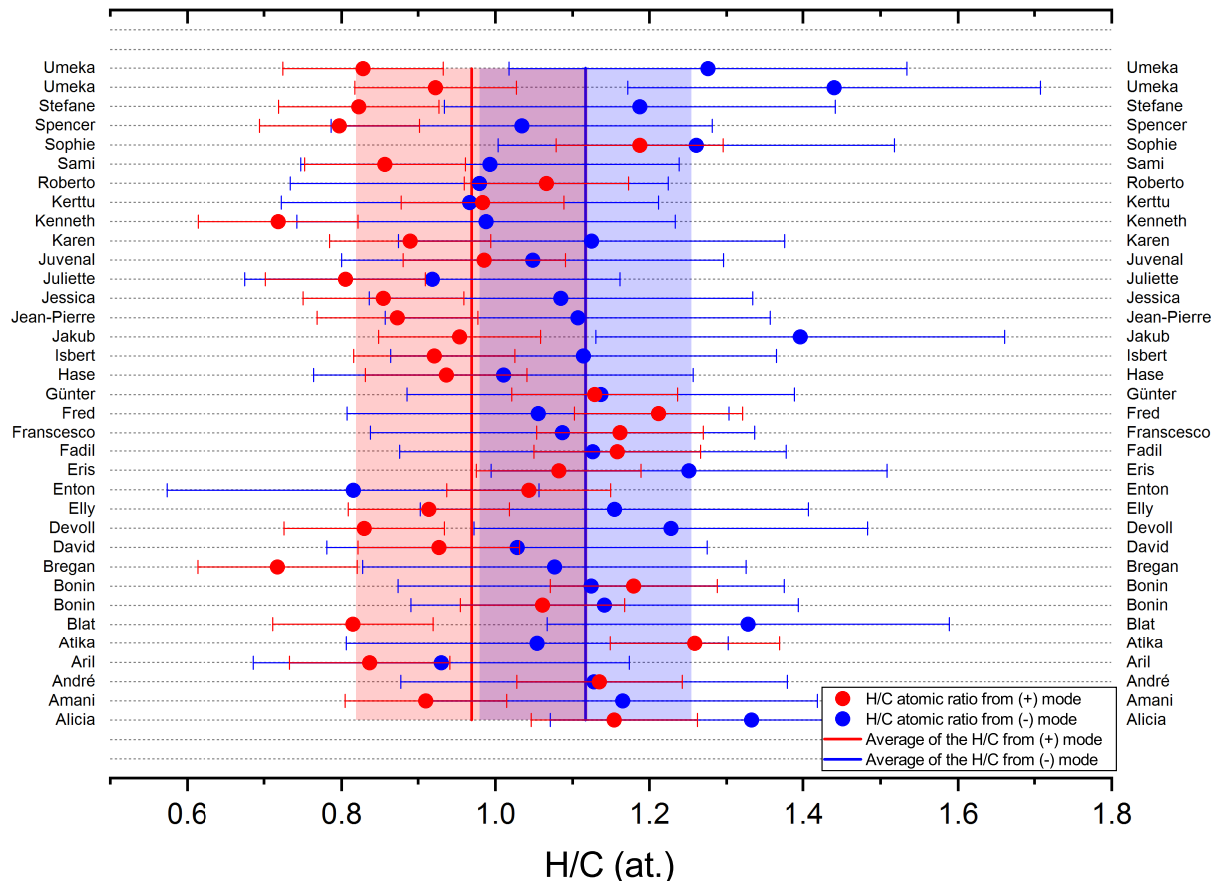


Fig. 3. H/C atomic ratios of the 35 considered analyses of the cometary particles arranged by alphabetic order. For each analysis (i.e., horizontal line), the red and blue points correspond to the H/C values obtained with the calibration curves (from positive- and negative-mass spectra, respectively). The two vertical lines represent the averages of the H/C atomic ratio for the two modes, the red and blue color bands are the associated 1σ standard deviations.

The H/C of the refractory organics in the particles is much lower than the H/C values (≥ 2) of the small volatile hydrocarbons (e.g., ethane, methanol, or glycine) that were detected in the gaseous coma of 67P (Le Roy et al. 2015b; Altwegg et al. 2016) by the Rosetta Orbiter Spectrometer for Ion and Neutral Analysis (ROSINA) instrument (Balsiger et al. 2007). This confirms that the refractory carbonaceous matter that dominates the cometary dust particles is chemically different from the molecules found in the gas phase of 67P.

Because the cometary particles were collected at different periods, we searched for correlations between the chemical composition and the collection date, as shown in Fig. 4. The goal was to determine whether the chemical composition of the dust evolved with the heliocentric distance at which the particles were collected. No such trend was observed. Between their collection and analysis, the particles remained inside the COSIMA instrument at temperatures of about 283 K. It is also possible that the particles contained volatile organic compounds (VOCs) when they were collected, and that these VOCs sublimated away during storage, thereby changing the H/C ratios of the particles with time. We therefore also tried to find a correlation between the H/C ratios and the time intervals between the collection and the analysis of the particles (see Fig. 5). Once again, no correlation is observed, and we conclude that the composition of the cometary particles did not vary during their 283 K storage.

To conclude, the H/C elemental ratio of the organic matter in cometary particles of 67P does not depend on their collection dates or their residence time before analysis. This H/C cometary

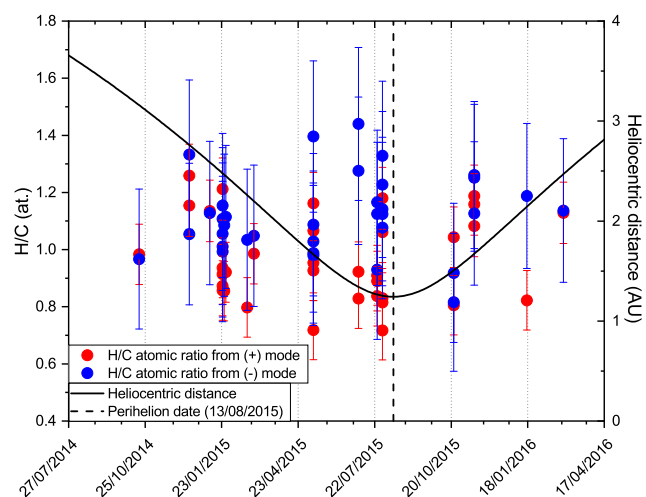


Fig. 4. H/C atomic ratio of the 35 considered analyses as a function of the collection date of the cometary particles for the two registration modes (red and blue points are positive and negative analyses, respectively). The black curve and the dashed line represent the heliocentric distance of 67P and the date at the perihelion (13 August 2015), respectively.

average of 1.04 ± 0.16 is in line with the assumption of Bardyn et al. (2017), confirming their estimate of the bulk elemental composition for the comet.

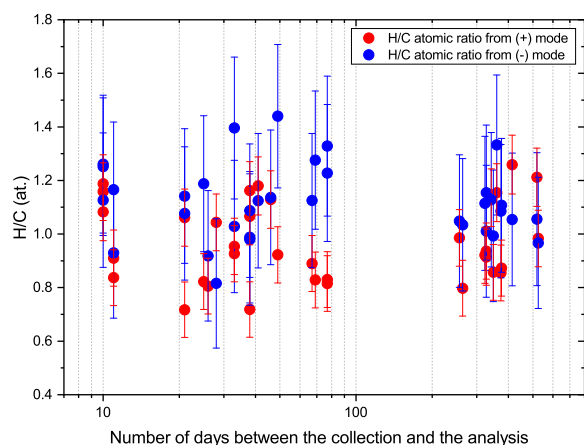


Fig. 5. H/C atomic ratio of the 35 considered analyses for the two registration modes (red and blue points are positive and negative analyses, respectively) as a function of the time between the collection date of the cometary particles and their analysis.

3.2. Comparison with other astrophysical objects and implications

The H/C atomic ratio measured in the particles of 67P can be compared to those found in other comets and in extraterrestrial materials available on Earth, such as meteorites, micrometeorites, and IDPs. The hydrogen of 67P particles is thought to be mainly contained in the organic phase because the COSIMA mass spectra show that the mineral phase is mostly anhydrous (Bardyn et al. 2017). Moreover, as no carbonates have been detected in the cometary particles so far, we assume that all the carbon is contained in the organic phase. Thus, the estimated H/C of the particles should be related to their refractory organic component.

The PUMA-1 mass spectrometer on board the Vega-1 spacecraft was able to measure an H/C ratio equal to 0.8 for the organic fraction of the Halley dust particles (Kissel & Krueger 1987). However, all the errors on the elemental ratios have been estimated to be on the order of a factor of 2, except for the hydrogen-to-silicon ratio, for which the uncertainty is unknown and could be higher (Kissel & Krueger 1987). For this reason, we must use caution when comparing this H/C value with the ratio measured for the cometary particles of 67P.

No reliable H/C value can be measured in the particles of Wild 2 because carbonaceous contaminants carrying CH₂ and CH₃ groups were present in the aerogel that collected the particles (Sandford et al. 2010). However, from the IR 3.4 μm band, Matrajt et al. (2013) showed that the cometary organic matter of Wild 2 particles resembles the organic component of IDPs, but differs from IOMs in that the CH₂ group is more abundant than the CH₃ group, leading to a lower CH₃/CH₂ ratio in Wild 2 particles than in the IOMs. This result suggests that Wild 2 samples (and IDPs), compared to the IOM of carbonaceous chondrites, have an organic component that is characterized by either longer or less branched aliphatic chains. CH₃/CH₂ ratios only give information about the aliphatic material and cannot be directly compared to the bulk H/C elemental ratio, which is related to the unsaturation of the whole organic component. Orthous-Daunay et al. (2013) indeed showed that the CH₃/CH₂ and H/C ratios in chondritic IOM are not correlated.

Flynn et al. (2003) detected more C=C functional groups in IOM than in IDPs. This observation implies that the H/C atomic ratios of IDPs are generally higher than those measured in IOMs. Nevertheless, aromatic materials, including a wide variety of

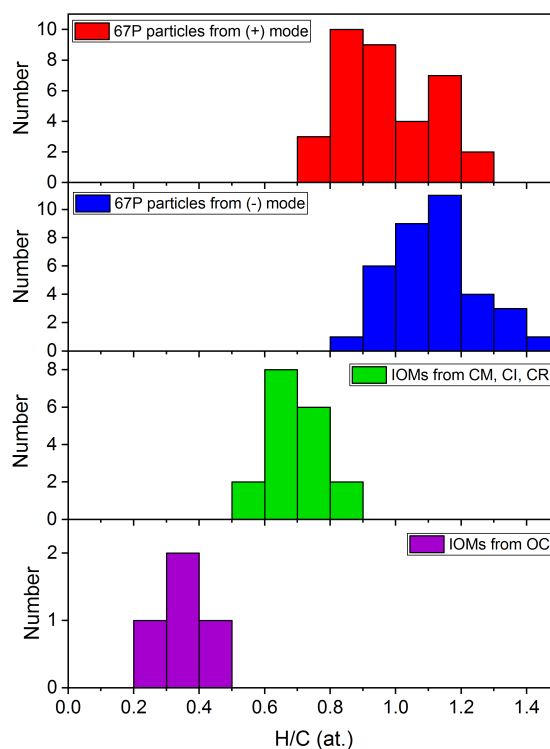


Fig. 6. Histograms of the H/C atomic ratios as deduced by COSIMA for 33 cometary particles of 67P for the ion registration mode (positive mode in red in the *first panel*, negative mode in blue in the *second panel*), and the H/C ratio measured in 22 IOM samples extracted from CI, CM, and CR carbonaceous chondrites (in green in the *third panel*) and in 4 IOM samples from ordinary chondrites (in purple in the *fourth panel*). All H/C atomic ratios of the IOM samples of chondrites were measured by Alexander et al. (2007).

PAHs, are suspected in IDPs (Clemett et al. 1993; Flynn et al. 2013). These highly unsaturated structures are also observed in micrometeorites (Clemett et al. 1998; Dobrică et al. 2011). The H/C atomic ratio can change dramatically across the surface (at a micrometric scale) of the same extraterrestrial particle (e.g., IDP or UCAMM) from 0.1 to 2 (Aléon et al. 2001; Duprat et al. 2010), suggesting that several organic phases are intermixed at a small spatial scale.

Because the IOMs extracted from meteorites are considered as the best analogs of the cometary organic matter of 67P so far (Fray et al. 2016), it is important to compare the H/C values between those two categories of extraterrestrial samples. The H/C atomic ratio has been measured in IOMs extracted from a wide range of chondritic meteorites (Alexander et al. 2007, 2010, 2014). We chose to compare the H/C atomic ratios of the cometary particles of 67P with the values found in the IOMs extracted from the least weathered and heated CM, CI, CR, and OC chondrites (see Fig. 6). The two distributions of the cometary H/C measured in positive and negative ionization registration modes are slightly different but may be comparable (most values are included in the 0.77–1.27 range; see Sect. 3.1). However, the elemental H/C ratios for the IOM samples mainly vary from 0.55 to 0.85 and from 0.05 to 0.55 for the IOMs extracted from CM, CI, CR, and those from OC chondrites, respectively (see Fig. 6). Consequently, the H/C atomic ratio is generally higher in cometary particles of 67P than in IOMs extracted from chondrites. This result implies that the refractory organic matter of the cometary particles of 67P is on average more hydrogenated and less unsaturated than the IOMs of even the most primitive chondrites.

Based on the discussion above, unsaturated materials seem to be present in the organic matter of all the studied astrophysical objects. However, these different samples can be classified based on the quantitative H/C atomic ratios or the qualitative measurements of aromatic and olefinic signatures. Thus, the IOMs extracted from carbonaceous chondrites are generally more unsaturated than the whole organic content of IDPs and cometary particles of 67P. Nevertheless, this does not mean that the particles of 67P and IDPs are similar. Different IDPs (possibly from different parent bodies) show considerable apparent diversity in the types of organic components, which range from a highly condensed material to a more aliphatic material (Aléon et al. 2001). This heterogeneity among the particles of 67P would probably not have been observed because it is probably present at a smaller spatial scale than the spatial resolution of COSIMA. Nevertheless, here we show that the organic matter of cometary particles of 67P remains broadly more hydrogenated and therefore less unsaturated than the meteoritic IOM.

4. Conclusions

For two years, the COSIMA mass spectrometer collected, imaged, and analyzed in situ the dust particles ejected from comet 67P/Churyumov-Gerasimenko. Using the two ionization registration modes, we found that the H^+/C^+ and H^-/C_2^- ratios were correlated with the H/C atomic ratio for a set of 14 calibration samples. We therefore generated two calibration lines that were used to measure the H/C elemental ratios of the organic matter contained in the cometary particles of 67P. By considering 33 cometary particles, the two mean H/C distributions overlap, and we estimated an average value of 1.04 ± 0.16 . The H/C ratio does not seem to be correlated to the collection date or to the residence time before analysis, suggesting that this refractory organic matter does not evolve throughout the cometary orbit and at the instrument temperature of around 283 K. The cometary H/C elemental ratios are most of the time higher than the values found in IOMs extracted from carbonaceous chondrites. This implies that cometary organic matter is less unsaturated than the matter found in chondritic IOMs.

The average value of 1.04 ± 0.16 for the H/C elemental ratio means that cometary organic matter remains highly unsaturated. Further work on the particles of 67P is necessary to characterize the chemical structure of this cometary organic component.

Acknowledgments. COSIMA was built by a consortium led by the Max-Planck-Institut für Extraterrestrische Physik, Garching, Germany, in collaboration with: the Laboratoire de Physique et Chimie de l'Environnement et de l'Espace, Orléans, France; the Institut d'Astrophysique Spatiale, CNRS/Université Paris Sud, Orsay, France; the Finnish Meteorological Institute, Helsinki, Finland; the Universität Wuppertal, Wuppertal, Germany; von Hoerner und Sulger GmbH, Schwetzingen, Germany; the Universität der Bundeswehr, Neubiberg, Germany; the Institut für Physik, Forschungszentrum Seibersdorf, Seibersdorf, Austria; and the Institut für Weltraumforschung, Österreichische Akademie der Wissenschaften, Graz, Austria; and is led by the Max-Planck-Institut für Sonnensystemforschung, Göttingen, Germany. We acknowledge the support of the national funding agencies of Germany (DLR, grant 50 QP 1302), France (CNES), Austria (project FWF P26871-N20), Finland and the ESA Technical Directorate. Rosetta is an ESA mission with contributions from its Member States and NASA. R.I. acknowledges support from the Labex Exploration Spatiale des Environnements Planétaires (ESEP; no. 2011-LABX-030). S.S. was funded by the Swedish National Space Board (contracts 121/11 and 198/15), the Swedish Research Council (contract 2015-04129).

References

Aléon, J., Engrand, C., Robert, F., & Chaussidon, M. 2001, *Geochim. Cosmochim. Acta*, **65**, 4399
 Alexander, C. M. O., Fogel, M., Yabuta, H., & Cody, G. D. 2007, *Geochim. Cosmochim. Acta*, **71**, 4380

Alexander, C. M. O., Newsome, S. D., Fogel, M. L., et al. 2010, *Geochim. Cosmochim. Acta*, **74**, 4417
 Alexander, C. M. O., Bowden, R., Fogel, M. L., et al. 2012, *Science*, **337**, 721
 Alexander, C. M. O., Cody, G. D., Kebukawa, Y., et al. 2014, *Meteorit. Planet. Sci.*, **49**, 503
 Altwegg, K., Balsiger, H., Bar-Nun, A., et al. 2016, *Sci. Adv.*, **2**, e1600285
 Bajt, S., Sandford, S., Flynn, G., et al. 2009, *Meteorit. Planet. Sci.*, **44**, 471
 Balsiger, H., Altwegg, K., Bochsler, P., et al. 2007, *Space Sci. Rev.*, **128**, 745
 Bardyn, A., Baklouti, D., Cottin, H., et al. 2017, *MNRAS*, **469**, S712
 Bentley, M. S., Schmied, R., Mannel, T., et al. 2016, *Nature*, **537**, 73
 Brownlee, D. 2014, *Annu. Rev. Earth Planet. Sci.*, **42**, 179
 Brownlee, D. E. 2016, *Elements*, **12**, 165
 Brownlee, D., Tsou, P., Aléon, J., et al. 2006, *Science*, **314**, 1711
 Carrasco, N., Jomard, F., Vigneron, J., Etcheberry, A., & Cernogora, G. 2016, *Planet. Space Sci.*, **128**, 52
 Clark, B. C., Mason, L. W., & Kissel, J. 1987, *A&A*, **187**, 779
 Clemett, S. J., Maechling, C. R., Zare, R. N., Swan, P. D., & Walker, R. M. 1993, *Science*, **262**, 721
 Clemett, S. J., Chillier, X. D. F., Gillette, S., et al. 1998, *Orig. Life Evol. Biosph.*, **28**, 425
 Cody, G. D., Alexander, C. M. O'D., & Tera, F. 2002, *Geochim. Cosmochim. Acta*, **66**, 1851
 Cody, G. D., Ade, H., Alexander, C. M. O'D., et al. 2008, *Meteorit. Planet. Sci.*, **43**, 353
 Dartois, E., Engrand, C., Duprat, J., et al. 2018, *A&A*, **609**, A65
 De Gregorio, B. T., Stroud, R. M., Cody, G. D., et al. 2011, *Meteorit. Planet. Sci.*, **46**, 1376
 Derenne, S., & Robert, F. 2010, *Meteorit. Planet. Sci.*, **45**, 1461
 Dobrică, E., Engrand, C., Quirico, E., Montagnac, G., & Duprat, J. 2011, *Meteorit. Planet. Sci.*, **46**, 1363
 Duprat, J., Dobrică, E., Engrand, C., et al. 2010, *Science*, **328**, 742
 Elsilá, J. E., Glavin, D. P., & Dworkin, J. P. 2009, *Meteorit. Planet. Sci.*, **44**, 1323
 Flynn, G. J., Keller, L. P., Feser, M., Wirick, S., & Jacobsen, C. 2003, *Geochim. Cosmochim. Acta*, **67**, 4791
 Flynn, G. J., Wirick, S., & Keller, L. P. 2013, *Earth, Planets, and Space*, **65**, 1159
 Flynn, G. J., Nittler, L. R., & Engrand, C. 2016, *Elements*, **12**, 177
 Fomenkova, M. N. 1999, *Space Sci. Rev.*, **90**, 109
 Fomenkova, N. M., Chang, S., & Mukhin, L. M. 1994, *Geochim. Cosmochim. Acta*, **58**, 4508
 Fray, N., Bardyn, A., Cottin, H., et al. 2016, *Nature*, **538**, 72
 Fray, N., Bardyn, A., Cottin, H., et al. 2017, *MNRAS*, **469**, S506
 Henkel, T., & Gilmour, J. 2014, *Treatise on Geochemistry*, 2nd edn. (Oxford: Elsevier), 411
 Hilchenbach, M., Kissel, J., Langevin, Y., et al. 2016, *ApJ*, **816**, L32
 Hilchenbach, M., Fischer, H., Langevin, Y., et al. 2017, *Phil. Trans. R. Soc. London, Ser. A*, **375**, 20160255
 Hornung, K., Kissel, J., Fischer, H., et al. 2014, *Planet. Space Sci.*, **103**, 309
 Hornung, K., Merouane, S., Hilchenbach, M., et al. 2016, *Planet. Space Sci.*, **133**, 63
 Jessberger, E. K., Christoforidis, A., & Kissel, J. 1988, *Nature*, **332**, 691
 Kissel, J., & Krueger, F. R. 1987, *Nature*, **326**, 755
 Kissel, J., Brownlee, D. E., Buchler, K., et al. 1986a, *Nature*, **321**, 336
 Kissel, J., Sagdeev, R. Z., Bertaux, J. L., et al. 1986b, *Nature*, **321**, 280
 Kissel, J., Altwegg, K., Clark, B. C., et al. 2007, *Space Sci. Rev.*, **128**, 823
 Langevin, Y., Hilchenbach, M., Ligier, N., et al. 2016, *Icarus*, **271**, 76
 Lawler, M. E., & Brownlee, D. E. 1992, *Nature*, **359**, 810
 Le Guillou, C., Remusat, L., Bernard, S., Brearley, A. J., & Leroux, H. 2013, *Icarus*, **226**, 101
 Le Roy, L., Bardyn, A., Briois, C., et al. 2015a, *Planet. Space Sci.*, **105**, 1
 Le Roy, L., Altwegg, K., Balsiger, H., et al. 2015b, *A&A*, **583**, A1
 Matrajt, G., Flynn, G., Brownlee, D., Joswiak, D., & Bajt, S. 2013, *ApJ*, **765**, 145
 Merouane, S., Stenzel, O., Hilchenbach, M., et al. 2017, *MNRAS*, **469**, S459
 Orthous-Daunay, F.-R., Quirico, E., Beck, P., et al. 2013, *Icarus*, **223**, 534
 Piani, L. 2012, Thesis, Museum national d'histoire naturelle - Paris, France
 Quirico, E., Orthous-Daunay, F.-R., Beck, P., et al. 2014, *Geochim. Cosmochim. Acta*, **136**, 80
 Reinhard, R. 1986, *Nature*, **321**, 313
 Rotundi, A., Sierks, H., Della Corte, V., et al. 2015, *Science*, **347**, aaa3905
 Sagdeev, R. Z., Blamont, J., Galeev, A. A., et al. 1986, *Nature*, **321**, 259
 Sandford, S. A., Bajt, S., Clemett, S. J., et al. 2010, *Meteorit. Planet. Sci.*, **45**, 406
 Sandford, S. A., Engrand, C., & Rotundi, A. 2016, *Elements*, **12**, 185
 Thomas, K. L., Blanford, G. E., Keller, L. P., Klock, W., & McKay, D. S. 1993, *Geochim. Cosmochim. Acta*, **57**, 1551
 Vickerman, J. C., & Briggs, D. 2013, *Tof-SIMS: materials analysis by mass spectrometry* (Chichester: IM Publications)
 Willacy, K., Alexander, C., Ali-Dib, M., et al. 2015, *Space Sci. Rev.*, **197**, 151

Appendix A: Fluorine contamination

A.1. Method

TOF-SIMS analyses of the IOMs derived from meteorites listed in Table 1 were performed on a TOF-SIMS IV instrument (ION-TOF GmbH, Germany) at the Department of Chemistry and Materials at RISE Research Institute of Sweden, Sweden. The analyses were made with a 25 keV Bi_3^+ beam at a pulsed current of 0.1 pA in high-mass resolution mode (bunched mode: $m/\Delta m \sim 3000\text{--}6000$ at $m/z = 30$, spatial resolution $\Delta l \sim 5 \mu\text{m}$) for 250–700 s on an area of 60×60 and $500 \times 500 \mu\text{m}$, depending on the size of the IOM. The sample surface was not flooded with electrons for charge compensation to simulate COSIMA measurements. All the data were saved as raw data files, which enables performing a retrospective analysis; that is, additional spectra, ion images, and profiles of the specific masses and regions of interest can be retrieved after the data acquisition is completed.

A.2. Discussion

The ion image of F^- obtained in the commercial TOF-SIMS measurement of IOMs clearly shows at least two fluorine-bearing phases in the IOMs (Fig. A.1). One phase is more diffuse and is found in the whole area of the IOMs, while the other phase is more localized and colocalized with the CF^+ signal,

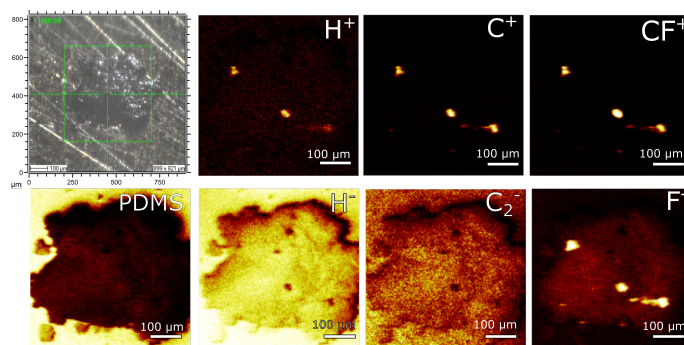


Fig. A.1. TOF-SIMS video and ion images of a small piece of IOM derived from GRO 95566 on a gold target 574. Ion images of H^+ , C^+ , CF^+ , PDMS ($\text{Si}(\text{CH}_3)_3^+$), H^- , C_2^- , and F^- ions are shown. The field of view of the ion images is $500 \times 500 \mu\text{m}$.

which probably originates from small flakes of an organofluorine contaminant. The CF^+ signal shows further colocalization with an increased intensity of H^+ and C^+ ion signals. This increased intensity of H^+ and C^+ ions in the contaminated areas most likely affects any H^+/C^+ ratio derived from these areas. We therefore only considered the spectra with a small number of counts for CF^+ and F^- ions to produce the calibration lines shown in Fig. 1 (see discussion in Sect. 2.2).

Appendix B: Additional table

Table B.1. Particles of 67 P considered for the measurements of their H/C atomic ratio.

#	Name	Target	Collection date	Analysis date (+)	Analysis date (-)	Residence time (days)	H ⁺ /C ⁺	H ⁻ /C ₂ ⁻	H/C (+)	H/C (-)
1	Alicia	1CF	2014-12-16	2015-12-11	2015-12-10	360	7.23 ± 0.05	107 ± 68	1.15 ± 0.11	1.33 ± 0.26
2	Amani	2CD	2015-07-25	2015-08-05	2015-08-06	11	6.07 ± 0.26	91 ± 21	0.91 ± 0.10	1.17 ± 0.25
3	André	1CF	2015-01-09	2015-12-17	2015-12-16	342	7.14 ± 0.06	88 ± 18	1.14 ± 0.11	1.13 ± 0.25
4	Aril	2CD	2015-07-25	2015-08-05	2015-08-06	11	5.73 ± 0.09	69 ± 14	0.84 ± 0.10	0.93 ± 0.24
5	Atika	1CF	2014-12-16	2016-02-03	2016-02-03	414	7.72 ± 0.04	81 ± 17	1.26 ± 0.11	1.05 ± 0.25
6	Blat	1CD	2015-07-31	2015-10-16	2015-10-15	77	5.63 ± 0.02	107 ± 7	0.82 ± 0.10	1.33 ± 0.26
7	Bonin	1CD	2015-07-31	2015-08-21	2015-08-20	21	6.79 ± 0.08	89 ± 8	1.06 ± 0.11	1.14 ± 0.25
8	Bonin	1CD	2015-07-31	2015-09-10	2015-09-09	41	7.35 ± 0.04	87 ± 45	1.18 ± 0.11	1.12 ± 0.25
9	Bregan	1CD	2015-07-31	2015-08-21	2015-08-20	21	5.17 ± 0.05	83 ± 13	0.72 ± 0.10	1.08 ± 0.25
10	David	2D1	2015-05-11	2015-06-13	2015-06-12	33	6.15 ± 0.04	78 ± 8	0.93 ± 0.10	1.03 ± 0.25
11	Devoll	1CD	2015-07-31	2015-10-16	2015-10-15	77	5.70 ± 0.01	97 ± 62	0.83 ± 0.10	1.23 ± 0.26
12	Elly	1CF	2015-01-24	2015-12-17	2015-12-16	327	6.09 ± 0.05	90 ± 39	0.91 ± 0.10	1.15 ± 0.25
13	Enton	1D2	2015-10-23	2015-11-20	2015-11-19	28	6.70 ± 0.09	57 ± 13	1.04 ± 0.11	0.82 ± 0.24
14	Eris	1D2	2015-11-16	2015-11-26	2015-11-25	10	6.89 ± 0.32	100 ± 10	1.08 ± 0.11	1.25 ± 0.26
15	Fadil	1D2	2015-11-16	2015-11-26	2015-11-25	10	7.25 ± 0.03	88 ± 17	1.16 ± 0.11	1.13 ± 0.25
16	Franscesco	2D1	2015-05-11	2015-06-18	2015-06-17	38	7.26 ± 0.07	84 ± 3	1.16 ± 0.11	1.09 ± 0.25
17	Fred	2CF	2015-01-24	2016-06-26	2016-06-23	519	7.50 ± 0.01	81 ± 2	1.21 ± 0.11	1.06 ± 0.25
18	Günter	1D2	2016-02-29	2016-04-15	2016-04-14	46	7.11 ± 0.04	89 ± 7	1.13 ± 0.11	1.14 ± 0.25
19	Hase	1CF	2015-01-24	2015-12-17	2015-12-16	327	6.20 ± 0.06	76 ± 27	0.94 ± 0.10	1.01 ± 0.25
20	Isbert	1CF	2015-01-28	2015-12-17	2015-12-16	323	6.13 ± 0.11	86 ± 29	0.92 ± 0.10	1.11 ± 0.25
21	Jakub	2D1	2015-05-11	2015-06-13	2015-06-12	33	6.28 ± 0.10	114 ± 3	0.95 ± 0.11	1.40 ± 0.27
22	Jean-Pierre	2CF	2015-01-24	2016-02-04	2016-02-04	376	5.90 ± 0.10	86 ± 3	0.87 ± 0.10	1.11 ± 0.25
23	Jessica	2CF	2015-01-26	2016-02-04	2016-02-04	374	5.82 ± 0.02	84 ± 3	0.85 ± 0.10	1.09 ± 0.25
24	Juliette	1D2	2015-10-23	2015-11-18	2015-11-18	26	5.58 ± 0.05	67 ± 4	0.81 ± 0.10	0.92 ± 0.24
25	Juvenal	3C7	2015-03-02	2015-11-13	2015-11-12	256	6.43 ± 0.04	80 ± 4	0.99 ± 0.11	1.05 ± 0.25
26	Karen	2CD	2015-07-25	2015-09-30	2015-09-30	67	5.98 ± 0.04	87 ± 5	0.89 ± 0.10	1.13 ± 0.25
27	Kenneth	2D1	2015-05-11	2015-06-18	2015-06-17	38	5.17 ± 0.06	74 ± 12	0.72 ± 0.10	0.99 ± 0.25
28	Kerttu	3D0	2014-10-18	2016-03-26	2016-03-26	525	6.42 ± 0.03	72 ± 1	0.98 ± 0.11	0.97 ± 0.24
29	Roberto	2D1	2015-05-11	2015-06-18	2015-06-17	38	6.81 ± 0.17	73 ± 5	1.07 ± 0.11	0.98 ± 0.25
30	Sami	2CF	2015-01-24	2016-01-08	2016-01-08	349	5.82 ± 0.19	75 ± 3	0.86 ± 0.10	0.99 ± 0.25
31	Sophie	1D2	2015-11-16	2015-11-26	2015-11-25	10	7.38 ± 0.06	101 ± 1	1.19 ± 0.11	1.26 ± 0.26
32	Spencer	3C7	2015-02-22	2015-11-13	2015-11-12	264	5.55 ± 0.11	79 ± 9	0.80 ± 0.10	1.03 ± 0.25
33	Stefane	2D2	2016-01-17	2016-02-11	2016-02-11	25	5.66 ± 0.05	93 ± 2	0.82 ± 0.10	1.19 ± 0.25
34	Umeka	1CD	2015-07-03	2015-08-21	2015-08-20	49	6.13 ± 0.31	118 ± 2	0.92 ± 0.10	1.44 ± 0.27
35	Umeka	1CD	2015-07-03	2015-09-10	2015-09-09	69	5.69 ± 0.07	102 ± 3	0.83 ± 0.10	1.28 ± 0.26

Notes. Columns are: the collection target, the collection starting date, the analysis date in both positive and negative registration modes, the total residence time (time between collection and analysis in positive mode), the H⁺/C⁺ and H⁻/C₂⁻ ion ratios, and the corresponding H/C atomic ratio.